Prelesional Events in Atherogenesis

Accumulation of Extracellular Cholesterol-Rich Liposomes in the Arterial Intima and Cardiac Valves of the Hyperlipidemic Rabbit

NICOLAE SIMIONESCU, MD, ELIZA VASILE, PhD, FLOREA LUPU, PhD, GABRIEL POPESCU, PhD, and MAYA SIMIONESCU, PhD

From the Institute of Cellular Biology and Pathology, Bucharest, Romania

Biochemical, physiologic, and ultrastructural modifications which appear in the aortic intima and atrioventricular valves before monocyte diapedesis and foam cell formation were investigated in rabbits fed a cholesterol-rich diet. In the first 2 weeks of the diet, while plasma β-VLDL cholesterol was increased up to 15-fold, the intima showed an enhanced uptake and deposition of dietary ^{3}H-cholesterol, ^{125}I-β-VLDL, and the fluorescent β-VLDL-1,1'-dioctadecyl-3,3,3',3'-tetramethylindocarbocyanine conjugate. β-VLDL-gold complex perfused *in situ* was transcytosed across endothelium by plasmalemmal vesicles. Concomitantly, within the intima, a progressive accumulation of extracellular densely packed uni- or multilamellar vesicles took place. These commonly occurred in cell-free subendothelial spaces and were not associated with any sign of cytolysis. In freeze-fracture preparations, these vesicles appeared as smooth surfaces, suggesting the absence of translamellar proteins. Upon incubation with filipin, these extracellular liposomes (EL) displayed characteristic ~20 nm filipin-sterol complexes, revealing the presence of preparations unesterified cholesterol in the phospholipid lamellas. EL deposition was paralleled by proliferation of basal lamina-like material, microfibrils, and proteoglycans, and continued to increase during foam cell formation. For the entire period of our experiments, the endothelium was morphologically intact, and no platelet involvement was detected. The results show that an early prelesional ultrastructural change in lesion-prone aortic and valvular areas is the accumulation of extracellular phospholipid liposomes rich in unesterified cholesterol. (Am J Pathol 1986, 123:109–125)

AS DOCUMENTED from studies on animal models of diet-induced hypercholesterolemia, during the development of the atherosclerotic plaque, the earliest change so far detected is the focal adherence of mononuclear cells to arterial endothelium, followed by their migration into the intima,[1-3] presumably in response to some chemotactic stimuli.[1,4] The activated monocyte-derived macrophages are progressively loaded with cholesteryl ester-rich inclusions to become the foam cells of the fatty streak.[1,2,5-8]

The subtle cellular and molecular events which occur within the arterial wall in hyperlipidemic animals before monocyte diapedesis and their possible links with the fatty streak formation are largely unknown.[9]

We have recently conducted experiments aimed at identifying and characterizing the biochemical and ultrastructural modifications which appear in the prelesional stage in vascular regions known to be prone to fatty plaque development. These studies, carried out on cholesterol-fed rabbits, have shown that as early as the second week of the diet, in the intima of the aortic arch and in the ventricular aspect of atrioventricular valves, there is a characteristic appearance and continuous deposition of lipid material organized as small (~100–300 nm) vesicles formed by phospholipid lamellas rich in unesterified cholesterol. Because of their apparent structure, we tentatively called these features "extracellular liposomes" (EL); their characteristics and possible physiopathologic significance are further discussed.

Supported by the Ministry of Education of Romania and by NIH Grant HL-26343.

Accepted for publication November 15, 1985.

Address reprint requests to N. Simionescu, Institute of Cellular Biology and Pathology, 8, B.P. Hasdeu Street, Bucharest-79691, Romania.

Materials and Methods

Animals and Diet

Sixty-two male adult chinchilla rabbits, 2–3 kg in body weight, were fed for 1–12 weeks a diet containing 0.5% cholesterol and 5% butter. Animals sacrificed weekly were examined along three lines of investigation: 1) level of plasma lipids, 2) lipid uptake and accumulation by the arterial wall, and 3) ultrastructure and lipid cytochemistry of arterial intima.

Plasma Lipid Analysis

β-very low density lipoprotein (β-VLDL) ($d < 1.006$ g/ml) was isolated from pooled hyperlipidemic rabbits sera by the methods of Havel et al[10] and Redgrave et al[11] and verified by immunoelectrophoresis. Cholesterol and triglyceride contents were determined enzymatically with the Sigma reagent kit.

Under individual variations, within 2 weeks, the animals developed a hypercholesterolemia (plasma cholesterol increased 7–15 times) characterized by the occurrence of β-VLDL as major cholesterol carrier[7] (see Results). Therefore, a special series of experiments were addressed to the uptake and accumulation of β-VLDL by the arterial wall.

Uptake of β-VLDL by the Artery Wall

Preparation of β-VLDL and Its Conjugates

β-VLDL ($d < 1.006$ g/ml) was obtained from pooled hypercholesterolemic rabbit sera by 18–24 hours ultracentrifugation in a 60 Ti rotor employing a discontinuous saline gradient.[11] β-VLDL was then dialyzed for 48 hours at 4 C against 154 mM NaCl containing EDTA, 0.05 mg/ml, pH 7.2, or against Dulbecco's phosphate-buffered saline (PBS). By negative staining with 2% aqueous solution of uranyl acetate, the particle dimension was found to be 30–80 nm. The ratio of mass protein content to mass cholesterol content decreased from 1:1.5–2.0 in the first week to 1:13 in the eighth and ninth weeks of diet.

^{125}I-β-VLDL was prepared by the ICl method of McFarlane.[12] The specific activity was 100–330 cpm/ng protein. About 97–98% of ^{125}I-β-VLDL was precipitable with 10% trichloracetic acid (TCA), and 2–3% was extractable with chloroform-methanol. The ^{125}I distribution on protein was ~85% on apoprotein B, ~14–15% on apoprotein E, with some traces on apoprotein C. Measurements were carried out in a Beckman-4000 Gamma Counter.

Labeling of β-VLDL With 1,1'-Dioctadecyl-3,3,3',3'-tetramethylindocarbocyanine perchlorate (DiI)

One milligram protein β-VLDL was added to 2 ml serum ($d > 1.25$ g/ml) and filtered through a 1.2-μ Millipore filter. Then 50 μl DiI in dimethylsulfoxide was added and gently vortexed, and the sterile mixture was incubated at 37 C for 16 hours. The mixture density was raised to 1.063 g/ml with solid KBr; then the β-VLDL–DiI conjugate was isolated by ultracentrifugation.[13]

Iodination of β-VLDL–DiI

^{125}I-β-VLDL-DiI was obtained by the ICl procedure of McFarlane.[12]

β-VLDL–gold complex was prepared by adsorbing on 5 nm colloidal gold particles β-VLDL (10 μg protein content/ml); the complex was then centrifuged on a cushion of 35% sucrose at 20,000 rpm on a JA-21 rotor in a Beckman centrifuge for 30 minutes. By negative staining (2% uranyl acetate) it was found that 1–4 gold particles were attached to 1 particle of β-VLDL.

Experiments With ^{125}I-β-VLDL

Weekly, normal and hyperlipidemic rabbits were injected with 0.3–0.5 mCi ^{125}I-β-VLDL (obtained from animals at the same stage of diet) and sacrificed after 24 hours. The blood and the thoracic aorta were collected and counted in a Beckman-4000 Gamma Counter. After thorough washing with PBS, segments of the thoracic aorta were either used as a whole or stripped of their adventitia. In some specimens, the intima was gently removed with a cotton swab and separately counted; the remaining media was also separately measured. In homogenates of media, the amount of radioactivity precipitable with 10% TCA was greater than 90%. The same values were obtained for intima.

Experiments With ^{125}I-β-VLDL-DiI

To visualize the tissue localization of the perfused ^{125}I-β-VLDL, the lipoprotein was concomitantly labeled with the fluorescent probe DiI. To avoid the massive DiI uptake by the liver *in vivo*, the experiments were carried out *in situ*.

Biweekly, normal and hyperlipidemic rabbits were anesthetized; and, by the procedure described below, the vasculature was cleared of blood by perfusion with Dulbecco's phosphate-buffered saline (PBS) supplemented with 1 mM $CaCl_2$ and 14 mM glucose. The thoracic aorta was catheterized and 8–10 ml of ^{125}I-β-VLDL–DiI in PBS (4–5 mg cholesterol/ml) were recirculated at 37 C for 1–2 hours in a closed circuit: left ventricle to thoracic aorta to peristaltic pump to left ventricle. The excess lipoprotein was washed by perfusion with PBS for 2–3 minutes. All perfusates were oxygenated. The aorta was removed and radioactivity counted, either as a whole vessel or the intima and the media separately (left after removal of adventitia). Small segments of the aortic arch, the proximal part of inter-

costal branches, and the distal part of the aorta were collected, fixed in 4% paraformaldehyde and 2% glutaraldehyde in 0.1 M HCl-Na cacodylate buffer, pH 7.2, for 30 minutes, then frozen in −170 C cold isopentane and stored in liquid nitrogen. Frozen pieces of tissue were mounted on Tissue Tek and cut at 8–10 μ. Sections picked up on gelatin-coated slides were washed with PBS and mounted in 90% glycerol in PBS. Some specimens were first incubated for 1–3 minutes with 10 μg/ml Nile red.[14] Sections for fluorescent microscopy were viewed with rhodamine filters and epifluorescent illumination.

Experiments With β-VLDL–Gold

Normal and hyperlipidemic rabbits were perfused in the same manner as in the experiments with ^{125}I-β-VLDL–DiI, but the probe used was β-VLDL–gold (E_{520} = 1.2) at 37 C for 15 minutes. After the excess tracer was washed out by perfusion with 20 ml PBS, the vessels were fixed *in situ* by perfusing a solution of 4% paraformaldehyde and 2% glutaraldehyde in 0.1 M HCl-Na cacodylate buffer, pH 7.2; then pieces of thoracic aorta were further prepared for electron microscopy.

Incorporation of Dietary ^{3}H-Cholesterol Into the Aorta

A group of rabbits were fed the hyperlipidemic diet for 10 or 25 days. Before experiments, all animals were fasted overnight. ^{3}H-cholesterol (Institute for Atomic Physics, Bucharest) in ethanol was sprayed onto the diet. Each rabbit was given in 40 hours 1.5 mCi ^{3}H-cholesterol incorporated into a 100-g diet. At 18 and 40 hours, blood samples were taken from the marginal ear vein. Under general anesthesia, the animal vasculature was cleared of blood by perfusion with PBS through the abdominal aorta with the vena cava caudalis as the outlet. After thorough washing, small pieces from coronaries or the inner convex part of the aortic arch (see Tissue Sampling) were collected and prepared by standard procedures for electron microscopy. After the adventitia was stripped off, the intima was carefully removed with a fine razor blade or a cotton swab. The wet weight of this material accounted for less than 1% of the total weight of the aorta. The intimal tissue was extracted overnight in 1–1.5 ml of 0.13 M Tris-HCl buffer, pH 7.2, containing 0.05% NaN_3. The media was minced with a McIlwain chopper and extracted in 10 ml of the above buffer. Each extract was centrifuged at low speed, and the supernate was saved. The pellet was extracted overnight with chloroform-methanol, and the chloroform phase was counted by spectrometry. The supernate was centifuged in a JA-21 rotor at 20,000 for 1 hour. The remaining liquid material was treated as blood plasma for obtaining lipoproteinlike material. Its density was raised to 1.21 g/ml with solid KBr. A gradient containing 1.5 ml of d = 1.21 g/ml of extracted material, 3 ml of d = 1.063 g/ml, 1 ml of d = 1.006 g/ml of NaCl solution containing 0.05% NaN_3 was constructed in nitrocellulose tubes for a SW 50.1 rotor. The material was centrifuged at 50,000 rpm for 3 hours, then collected by puncturing the tube bottom. Plasma collected from the same animals was treated in the same way.

Electron Microscopy

At the time of the weekly sacrifice of normal and hyperlipidemic animals, segments of the aortic arch, thoracic aorta, and atrioventricular valves were prefixed by rapid immersion in 2% glutaraldehyde in 0.1 M HCl-Na cacodylate buffer, pH 7.4, at 22 C for 10 minutes. Both right and left atrioventricular valves were removed with their fibrous rings (to allow the identification of the valves' atrial and ventricular aspects), then dissected and further processed for thin-section or freeze-fracture electron microscopy.

Thin Sections

Samples were fixed for 90 minutes in 2% glutaraldehyde, postfixed for 90 minutes in 1% OsO_4, and mordanted with 1% tannic acid, all in 0.1 M HCl-Na cacodylate buffer.[15] Some specimens were fixed with the triple fixative solution containing 3 volumes of 5% paraformaldehyde, 2 volumes of 4% OsO_4, and 1 volume of saturated solution of lead citrate, all in 0.1 M HCl-Na cacodylate buffer. The mixture was freshly prepared on ice.[16] Other samples were fixed only with 6% OsO_4 in 0.1 M veronal-acetate buffer, pH 7.4. All specimens were dehydrated in graded ethanols and embedded in Epon 812. Sections cut on a Reichert Om3 or American Optical Ultracut microtomes were stained with 0.5% uranyl acetate and lead citrate.

To visualize the proteoglycans, we fixed some aortic segments in 2% glutaraldhyde in 0.1 M Sorensen's sodium phosphate buffer, pH 7.4, containing 0.1% safranin O, at room temperature. After thorough rinsing in phosphate buffer containing 0.2 M sucrose and 0.05% safranin O, specimens were postfixed in 1% OsO_4 in 0.1 M sodium phosphate buffer containing 0.025% safranin O.[17] After a rinse in phosphate buffer, then in 0.1 M HCl-Na cacodylate buffer, the samples were mordanted with tannic acid[15] and further processed for Epon embedding.

Freeze-Fracture

Specimens cryoprotection was done by treatment for 2 h with 25% glycerol in 0.1 M HCl-Na cacodylate buffer, pH 7.2. Specimens were then frozen in Freon 22 cooled with liquid nitrogen. The fracturing was per-

formed in a Balzers BAF 301 apparatus at −115 C in a vacuum better than 2×10^{-6} Torr. The platinum shadowed replicas were cleaned in Chlorox, rinsed in distilled water and mounted on coated 150-mesh grids. Both thin sections and replicas were examined with Philips HM 400 electron microscopes.

Lipid Histochemistry and Cytochemistry

Sampling for morphologic studies was based on observations made in a previous series of experiments, which indicated that in our experimental model the arterial regions most frequently (> 95%) affected by fatty-streak formation were the inner convex surface of the aortic arch and the ventricular aspect of the atrioventricular valves. The convex luminal region ("lesser curvature") of the aortic arch could be reliably used as a lesion-prone area for detecting very early biochemical or ultrastructural changes which might appear in the arterial intima before monocyte adhesion and diapedesis, therefore prior to any morphologically distinguishable lesion, such as fatty dots.

The further development of lesions such as the fatty streak was in parallel examined in similar lesion-prone areas of the aortic arch. The present study, however, was focused in particular on prelesional subtle changes which precede monocyte-macrophage diapedesis and foam cell formation.

Light Microscopy

Specimens were fixed by immersion in 10% formaldehyde in phosphate-buffered saline, pH 7.4, for 1 hour at 22 C, then frozen in isopentane cooled with liquid nitrogen, and cryosectioned.

Oil red O staining was used for detecting hydrophobic lipids, which presumably include some of the esterified cholesterol.[18-20] Sections were washed in propyleneglycol for 2 minutes, then immersed for 30 minutes in 0.5% oil red O (Serva, Heidelberg, West Germany) in propyleneglycol, washed three times in 70% propyleneglycol, 15 minutes in running water, and stained with Harris' hematoxylin for 5 minutes.

Nile red staining was performed as an alternative to the latter[14]: after sections were incubated for 5 minutes in 1 μg/ml Nile red in PBS (prepared by G. Popescu from Nile blue chloride, Loba Chemie, Vienna, Austria, according to Greenspan et al[14]) and briefly rinsed in PBS, they were examined by fluorescent microscopy with rhodamine filters.

Filipin, a fluorescent polyene antibiotic (a gift from Dr. J. Grady, Upjohn Co., Kalamazoo, Mich) was used for its reported specific binding to 3β-hydroxy sterols[21-23] to detect the unesterified cholesterol. One milligram of filipin dissolved in a drop of dimethylsulfoxide (Sigma, St. Louis, Mo) was added to 5 ml PBS, then layered over frozen sections for 30 minutes in a dark humidified chamber. After rinsing in PBS and mounting in glycerol, the specimens were examined and photographed in brightfield, phase-contrast, and fluorescence microscopy with a Fluoval fluorescence microscope (Karl Zeiss, Jena, East Germany). Filipin dye was excited by transillumination with ultraviolet light (UGI filter) from a 100-watt mercury lamp and viewed through a 510-nm barrier filter.

Electron Microscopy—Filipin

Specimens prefixed with 2% glutaraldehyde in 0.1 M HCl-Na cacodylate buffer, pH 7.4, for 10 minutes were incubated in the same fixative containing 0.02 mg/ml filipin, for 30–60 minutes at 22 C.

Thin Sections

Aldehyde fixation was completed to 40–60 minutes, followed by postfixation in 1% OsO_4 in 0.1 M HCl-Na cacodylate buffer for 90 minutes at 4 C, mordanting with tannic acid,[15] and further processing for electron microscopy.

Freeze-Fracture

Filipin-incubated specimens were cryoprotected with 25% glycerol in 0.1 M HCl-Na cacodylate buffer for 2 hours at 4 C, then frozen on gold carriers in Freon 22 cooled with liquid nitrogen; fracturing and shadowing in a Balzers BAF 301 apparatus.

Results

General

Our observations were extended over 12 weeks of hyperlipidemic diet. According to the findings obtained in a first series of experiments, the current investigations were focused on two early periods, described as follows:

1. Arbitrarily, we have designated as "prelesional" the stage preceding monocyte diapedesis into the vessel wall (with subsequent initiation of foam cell formation, smooth muscle cell involvement, stromal hyperplasia). In our experimental conditions, with relatively large individual variations, this period when no lesions (such as fatty dots) could be microscopically detected was usually 2 weeks.

2. After 2 weeks, monocytes started emigrating, and a progressive formation of foam cell occurred first in the intima of the aortic arch (the inner convex area) and the ventricular region of the atrioventricular valves of the heart. These two regions were selected as the most lesion-prone areas (>95%), and this was consistently confirmed in our experiments.

For the prelesional stage, the *in vivo* injection of Evans blue for depicting sites of increased permeability gave no reproducible results in rabbits (A. Radu, personal communication).

Because of the focal and heterogeneous character of the atherosclerotic lesions in general, in animals at 4–8 weeks of the diet we could observe coexisting regions of "prelesional" type, with areas in various stages of foam cell formation.

Serum Lipid and Lipoprotein Analysis

As compared with control animals in which the plasma cholesterol had an average of 0.31 mg cholesterol/ml serum, after 2 weeks of the diet this figure increased about 7–15 times, and in the eighth week and later reached values ~30–50 times higher than normal. In parallel with a progressive and drastic decrease in low density lipoprotein (LDL) content, the β-VLDL became the major cholesterol carrier. The ratio of mass protein content to mass cholesterol content diminished from 1:1.5–2.0, in the first week of the diet, to 1:13 in the eighth to ninth week of the diet (Figure 1).

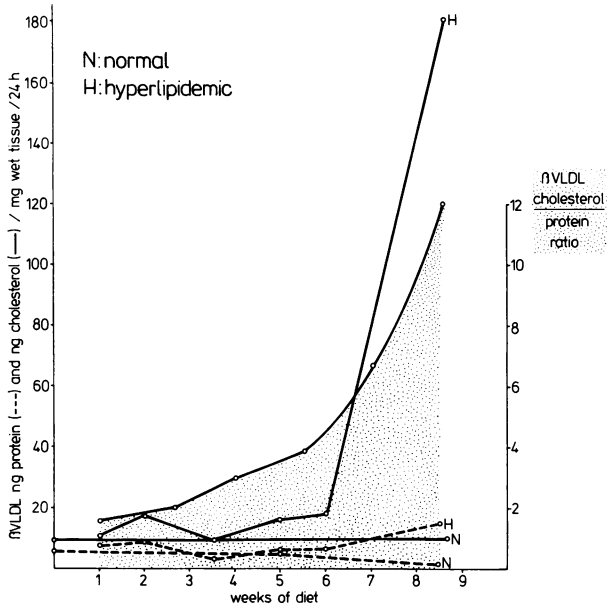

Figure 1—The uptake and accumulation by the aorta of normal and hyperlipidemic rabbits of ^{125}I-β-VLDL injected *in vivo* at different times during the diet and allowed to circulate for 24 hours.

Uptake and Accumulation of β-VLDL by the Artery Wall

As indicated by the experiments with ^{125}I-β-VLDL, in the first two weeks of diet, as compared with controls, in the aortic wall there was a slight deposition of β-VLDL protein, which at later stages remained at values very close to those found in normal rabbits. Conversely, because of the steep augmentation in the cholesterol content of β-VLDL particles (the cholesterol/protein ratio increased from 1.54:1 in the first week to 3.8:1 in the fifth week, and to 12.0:1 in the eighth week), a marked accumulation of cholesterol in the aortic wall of hyperlipidemic animals became evident (Figure 1).

In vivo and *in situ* uptake of β-VLDL double-labeled with ^{125}I and the fluorescent probe DiI by the aorta of normal rabbits remained constant at 10–15 ng cholesterol/mg aortic wet tissue per day. However, in the hyperlipidemic animals, the uptake increased progressively to reach 170–180 ng β-VLDL cholesterol/mg wet tissue/24 hours in the eighth and ninth weeks of the diet (Figure 1). Fifty to sixty percent of radioactivity was located in the intima. In contrast to controls, in frozen sections of the aorta of hyperlipidemic rabbits, the fluorescent β-VLDL–DiI material accumulated progressively in the intima (Figure 2).

At the cellular level, during the period examined (first 2 weeks), the β-VLDL–gold complexes were always found in endothelial structures involved in endocytosis, and especially in features potentially performing transcytosis, ie, plasmalemmal vesicles (Figure 3). Particles were also detected in subendothelium, but quantitative morphometry was not carried out on this material, which was basically intended to visualize the transendothelial pathway taken by this probe. No open junctions were seen, and no β-VLDL complexes could be encountered within intercellular spaces or junctions of aortic endothelium.

Incorporation of Dietary ^{3}H-Cholesterol Into the Aortic Wall

After 40 hours of the ^{3}H-cholesterol-containing diet, the radioactivity was recovered mainly in the serum β-VLDL fraction and to a lesser extent in the LDL fraction.

Although the intima represents less than 1% of the total weight of the wet aortic wall, 50–60% of the total dietary ^{3}H-cholesterol was recovered from the intima.

The level of radioactivity incorporated into the aortic intima of animals fed the hypercholesterolemic diet 10 days was comparable to the values of radioactivity detected in the intima of normal animals (~910 cpm versus 1000 cpm, respectively).

In rabbits fed the hypercholesterolemic diet for 25 days, the radioactivity incorporated into the aortic intima was almost double (~1900 cpm) the value obtained both in normal or 10-day diet-fed animals.

After ultracentrifugation, the material extracted from intima of both normal and hyperlipidemic rabbits was

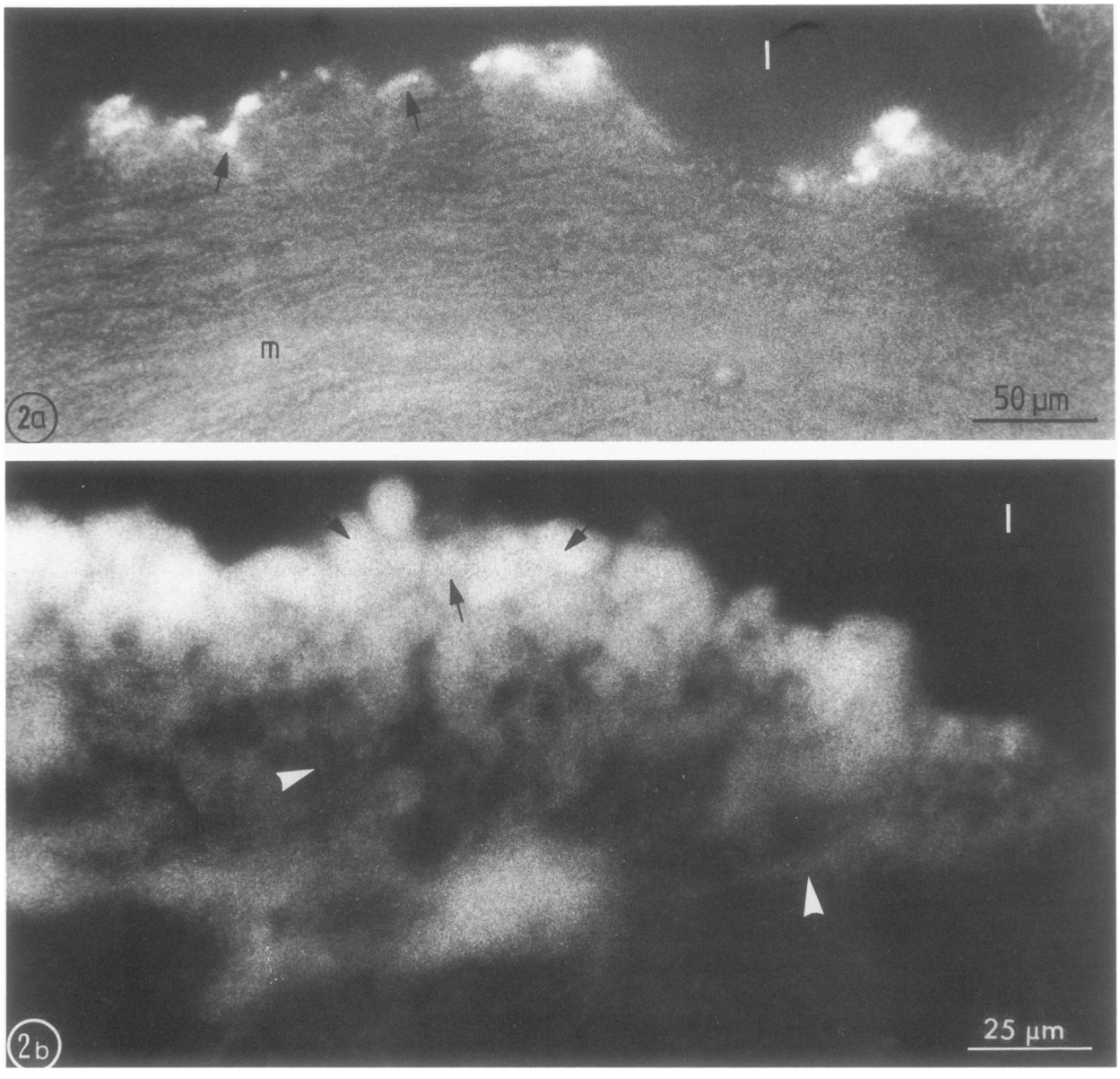

Figure 2—Frozen sections of the aortic wall of hyperlipidemic rabbits perfused *in situ* with β-VLDL–DiI for 2 hours at 37 C; specimens examined with rhodamine filters and epifluorescent illumination. **a**—At 2 weeks of the diet, β-VLDL–DiI (*arrows*) accumulates in the superficial area of the intima, which is devoid of grossly visible fatty dots; the media (*m*) lacks fluorescent material. (×385) **b**—At later stages, during foam cell formation in the intima, excess fluorescent lipidic material is deposited both intracellularly (*arrows*) and extracellularly (*arrowheads*). *I*, lumen. (×7700)

recovered as a very fine band located in the range density of LDL and β-LDL. This material is now under investigation.

Ultrastructural Changes: Lipid Histochemistry and Cytochemistry

Control Animals

The aortic initima of normal rabbits commonly consists of endothelium, basal lamina, subendothelial matrix containing collagen fibers, bundles of elastin, microfibrils, and proteoglycans, and lamina elastica interna. Occasionally macrophages and some leukocytes may be found in this location. A relatively similar structure can be ascribed to the ventricular region of the atrioventricular valves, except for the elastic elements, which are rather rare. In both locations, only occasionally could a few extracellular small vesiclelike features be observed.

Prelesional Stage

In the first 2 weeks of hyperlipidemic diet, no detectable alterations could be observed in the vascular areas as examined by light microscopy and lipid histochemis-

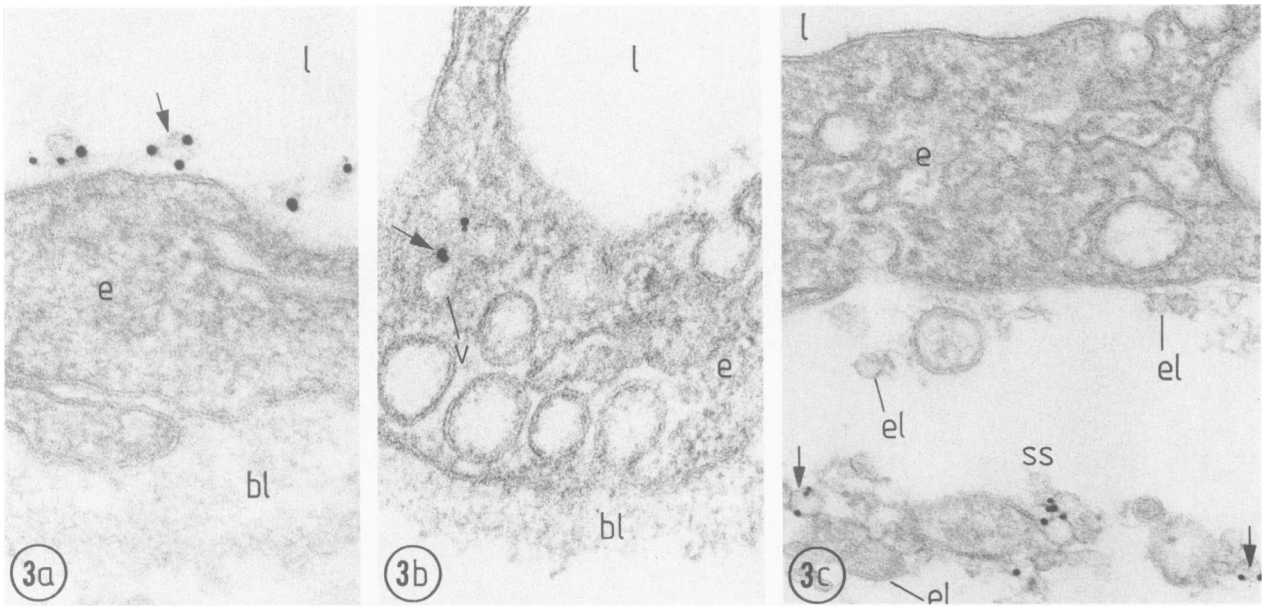

Figure 3—Aortic endothelium of hyperlipidemic rabbits after perfusion *in situ* of β-VLDL–gold complex (β-VLDL-Au). The complex particles (*arrows*) can be seen either close to plasma membrane (**a**), within plasmalemmal vesicles (**b**), or in the subendothelial space (**c**), where they may be associated with polymorphic vesicles, presumably extracellular liposomes (*el*). *l*, lumen; *e*, endothelium; *v*, plasmalemmal vesicles; *ss*, subendothelial space. Notice the dissolution of basal lamina in areas of EL accumulation. (**a**, ×108,000; **b**, ×110,000; **c**, ×80,000)

try after staining with Nile red or oil red O. Upon incubation with filipin, fluorescent material became visible in the intima at about 2–3 weeks of the diet, but its intracellular or extracellular location was difficult to assess. The results obtained with Nile red O were largely comparable to those revealed by DiI-conjugated β-VLDL (Figure 2). At about 4 weeks of the diet, oil red-positive material was also detectable within the intima.

In similar, apparently lesion-free specimens, the electron microscopy revealed the existence within the matrix of the intima of numerous, relatively densely packed unilamellar and multilamellar vesicles about 100–300 nm in diameter, which we tentatively called "extracellular liposomes". In chemically fixed specimens processed for transmission electron microscopy by the standard procedure, ELs appeared to be constituted by phospholipid lamellae, particularly well preserved after mordanting the specimens with tannic acid. Some ELs had on a part of their contours several tightly packed lamellas and only one or two lamellas on the rest. ELs did not contain in their interior an electron-dense material. Initially, when in small number, ELs appeared in the subendothelium, sometimes interposed between endothelium and its basal lamina, which seemed to be progressively detached, and new basal lamina-like material formed. When in large number, ELs had the tendency to accumulate against elastica interna, being also closely associated with microfibrils and proteoglycans (Figure 4). At this stage, in those intimal areas there were not any signs of cytolysis; moreover, endothelium was always morphologically intact, without any image of blebbing.

The progressive accumulation of ELs coexisted with the proliferation of basal lamina-like material (particularly prominent in valves), microfibrils, and proteoglycans (Figure 4).

In freeze-fracture preparations, ELs appeared as rounder, smooth vesicles made up by one or more lamellas devoid of particles (Figure 5).

In specimens incubated with filipin, ELs displayed characteristic deformations expressing filipin-sterol complexes, visible both in thin sections (Figure 6), and freeze-fracture replicas (Figure 7). Early deposits detected by filipin could also be seen by fluorescent microscopy (Figure 6, inset). This indicated that the ELs contained within their lamellas (presumably phospholipids) various amounts of trapped unesterified cholesterol. No significant number of apparently intact lipoprotein particles (morphologically detectable because of their shape, size, and electron density) could be encountered.

Foam Cell Formation

Intimal accumulation of ELs was a continuous and progressive process, becoming particularly prominent during monocyte diapedesis, macrophage transformation, and their loading with lipid (4–8 weeks of the diet). The number of ELs became so salient in some areas that they virtually occupied completely the extracellular compartment between endothelium,

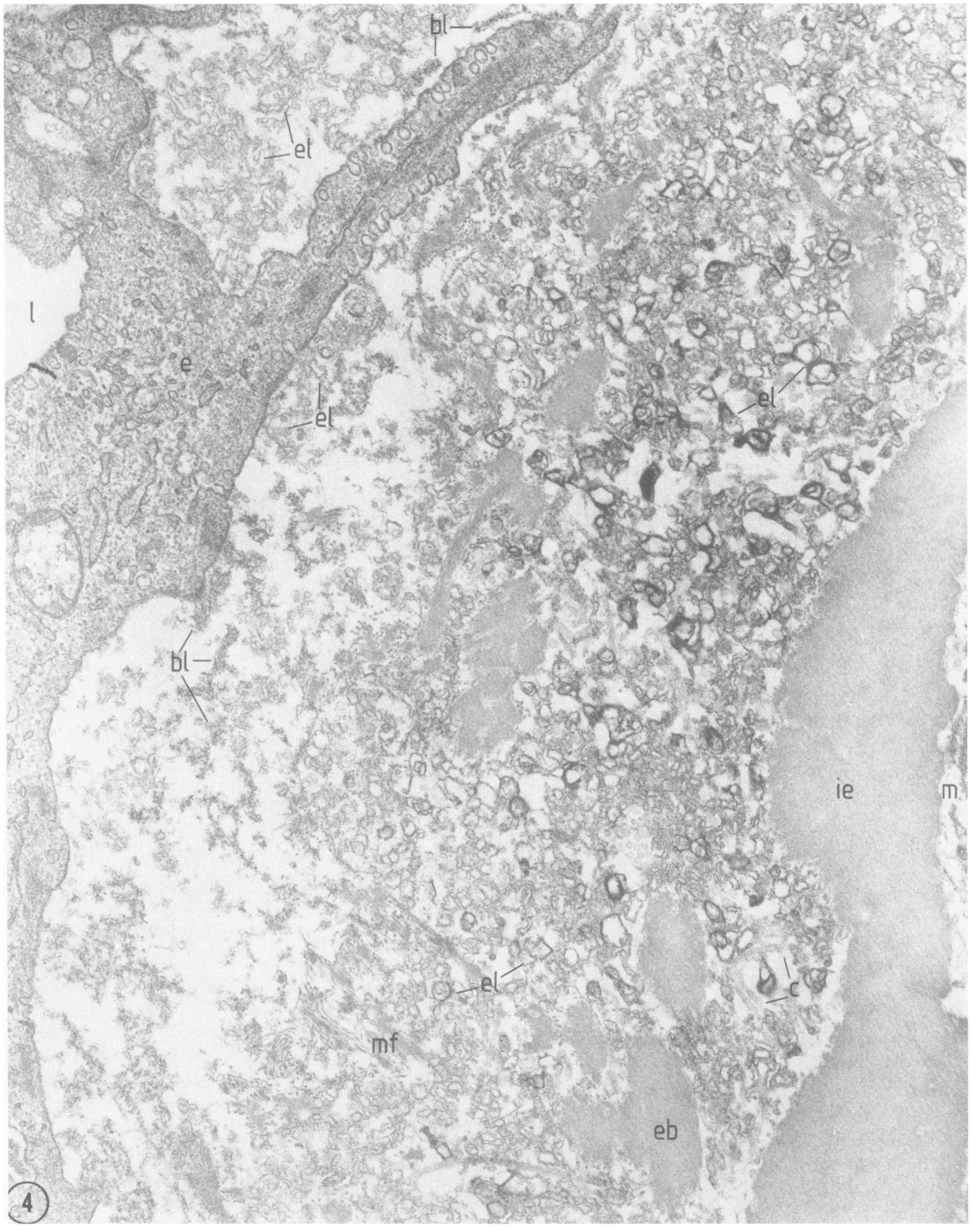

Figure 4—The inner convex region of the aortic arch of a hyperlipidemic rabbit at 2 weeks of the diet. The intima contains extracellular liposome-like vesicles (*el*) associated especially with microfibrils (*mf*), elastic bundles (*eb*), and internal elastica (*ie*). Basal lamina-like material (*bl*) is present in subendothelium. Groups of small extracellular liposomes (*el*) can also be seen interspersed among this material and focally between endothelium (*e*) and its disorganized basal lamina. Endothelium is structurally intact. *l*, lumen; *m*, smooth muscle cell of the media; *c*, collagen. (×28,000)

Figure 5—Freeze-fracture replica of a specimen similar to that in Figure 4. In *e*, an endothelial cell; the subendothelial space is occupied by densely packed, apparently unilamellar or multilamellar extracellular liposomes (*el*). *eb*, elastic bundles. (×76,000) **Inset**—The extracellular liposomes (*el*) have a smooth cleavage plane devoid of intralamellar particles. (×152,000)

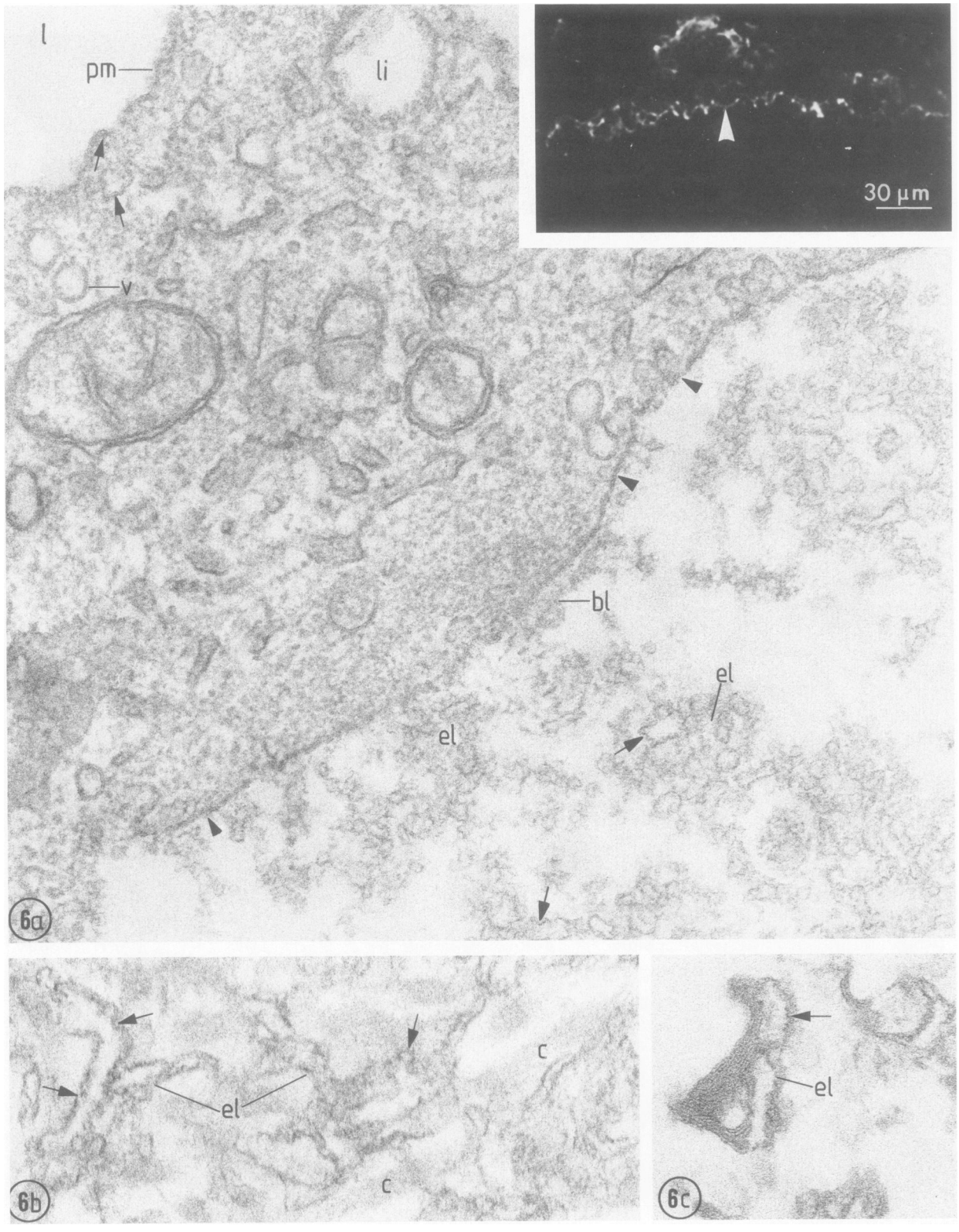

Figure 6a–c—Specimen similar to that depicted by Figure 4, incubated with filipin. Plasma membrane (*pm*) and vesicle membrane (*v*) of the endothelial cell as well as the extracellular liposomes (*el*) display characteristic deformations produced by filipin–sterol complexes (*arrows*, in **a** and **b**). In **a**, notice the disorganization of basal lamina (*bl*) at the sites of *EL* accumulation (*arrowheads*). **c**—A multilamellar liposome which developed filipin–sterol complexes only in the region formed by two lamellas (*arrow*). **Inset**—Early accumulation of fluorescent-positive material (filipin) (*arrowhead*) occurs in the intima, especially against elastica interna. *l*, lumen; *c*, collagen; *li*, lipid inclusion. (**a**, ×85,000; **b**, ×128,000; **c**, ×128,000)

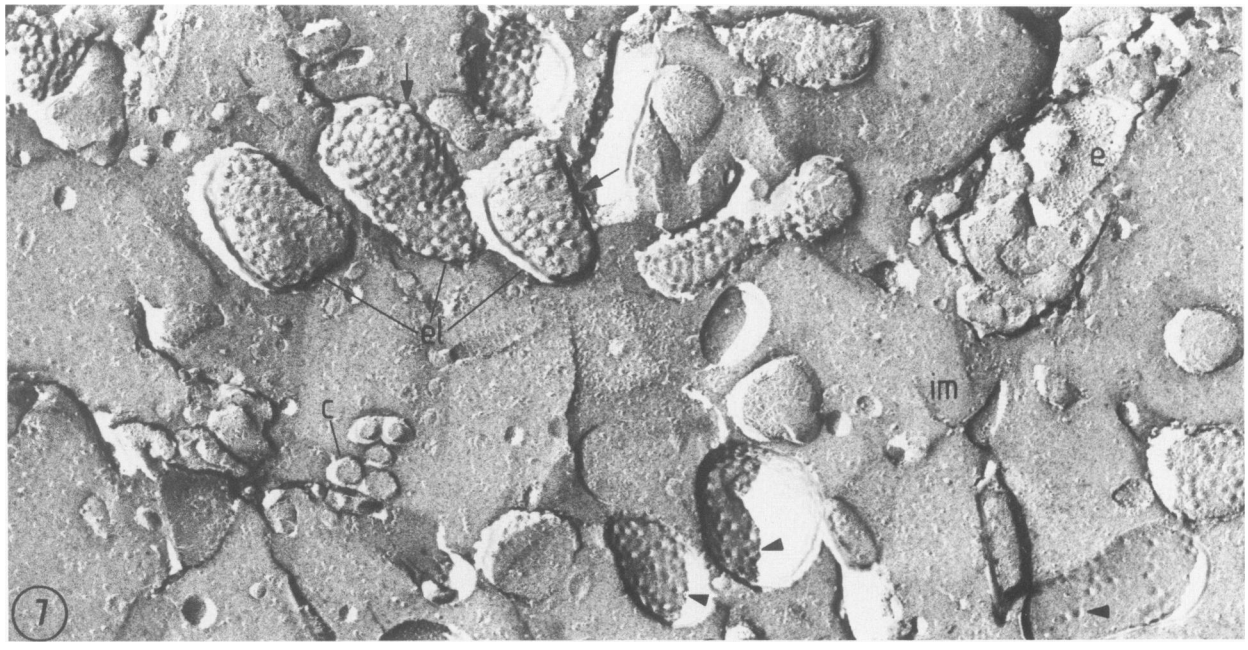

Figure 7—Upon incubation with filipin, almost all extracellular liposomes (*el*) develop filipin–sterol complexes, appearing in freeze-fracture preparations as characteristic ~20-nm protrusions (*arrows*) or pits (*arrowheads*). *c*, collagen; *e*, an abluminal extension of an endothelial cell; *im*, interstitial matrix. (×47,000)

elastica interna, and the interposed foam cells (Figure 8). At this stage, by fluorescence microscopy it could be easily seen the increasing deposition in the intima of DiI-positive and filipin-positive materials (Figures 2a and 6, inset, respectively). Filipin treatment revealed typical filipin–sterol complexes, both in thin-sectioned (Figure 9) and freeze-fractured samples (Figure 10).

With the increasing numbers and size of macrophage-derived and, at a later stage, smooth muscle-derived foam cells, the extracellular compartment was reduced in size, and so was the fractional volume occupied by ELs. When obvious processes of cytolysis were added to the lesion, the associated vesiclelike structures were very polymorphic, and their origin could not be assessed with certainty, but at that stage many of these vesicles appeared derived from cell debris.

ELs could also be seen in cell-free intimal regions located in the vicinity of a fatty streak or more advanced plaque.

Discussion

Most investigators consider the fatty streak as the earliest atherosclerotic lesion[24,25] characterized by the presence of cholesterol ester-rich foam cells[26,27] resulting mainly from monocyte-derived macrophages.[1,2] In response to some chemotactic stimuli,[4] these cells adhered to endothelium and emigrated into the intima,[1,2] where presumably they ingest modified low density lipoproteins via receptor-mediated uptake.[8] During these early events, no endothelial denudation and no platelet intervention was observed,[2,3,9] thus making questionable the validity of the "endothelial injury" hypothesis in its various forms[29–31] as the initiating factor in atherogenesis.

In the lesion-prone areas, more subtle changes which precede monocyte diapedesis and subsequent foam cell formation are poorly understood. Observations so far reported resulted usually from nonsystematic approaches in experimental hypercholesterolemia; they brought to attention focal endothelial changes associated with atherosclerotic tendencies such as increased thymidine uptake,[32] increased permeability to plasma proteins,[1,33] accumulation of IgG in endothelial cell,[34] reduction in cationic ferritin binding and in ruthenium red and Con A staining,[35–37] and increase in the number of endothelial cell vesicles and transendothelial channels,[38] breaks of endothelial junctions, and holes in endothelial cells.[39] Such modifications could not be convincingly related to other steps known to lead to plaque formation.

Our present results indicate that during the first 2 weeks of diet-induced hypercholesterolemia in rabbits, before monocyte diapedesis and formation of lipid-laden cells, more subtle changes occur in lesion-prone areas such as the aortic arch, coronary arteries (not described here), and atrioventricular valves. While plasma cholesterol, predominantly contained in the β-VLDL

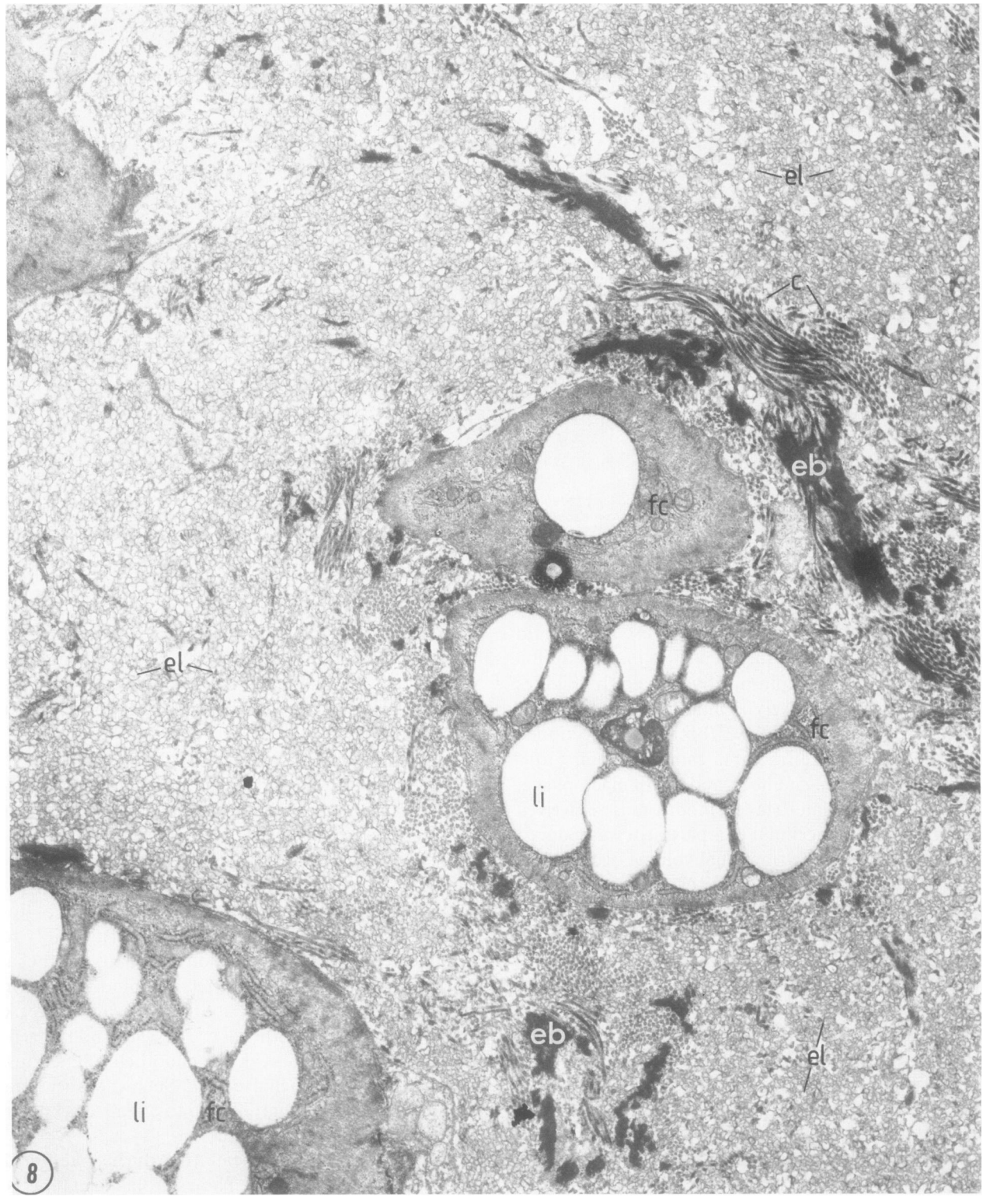

Figure 8—At 8 weeks of the diet, the aortic intima of the hyperlipidemic rabbits contains a remarkable amount of almost uniform extracellular liposomes (*el*), virtually filling completely the interstitial spaces between foam cells (*fc*). *eb*, elastic bundles; *c*, collagen; *li*, lipid inclusions. (×13,000)

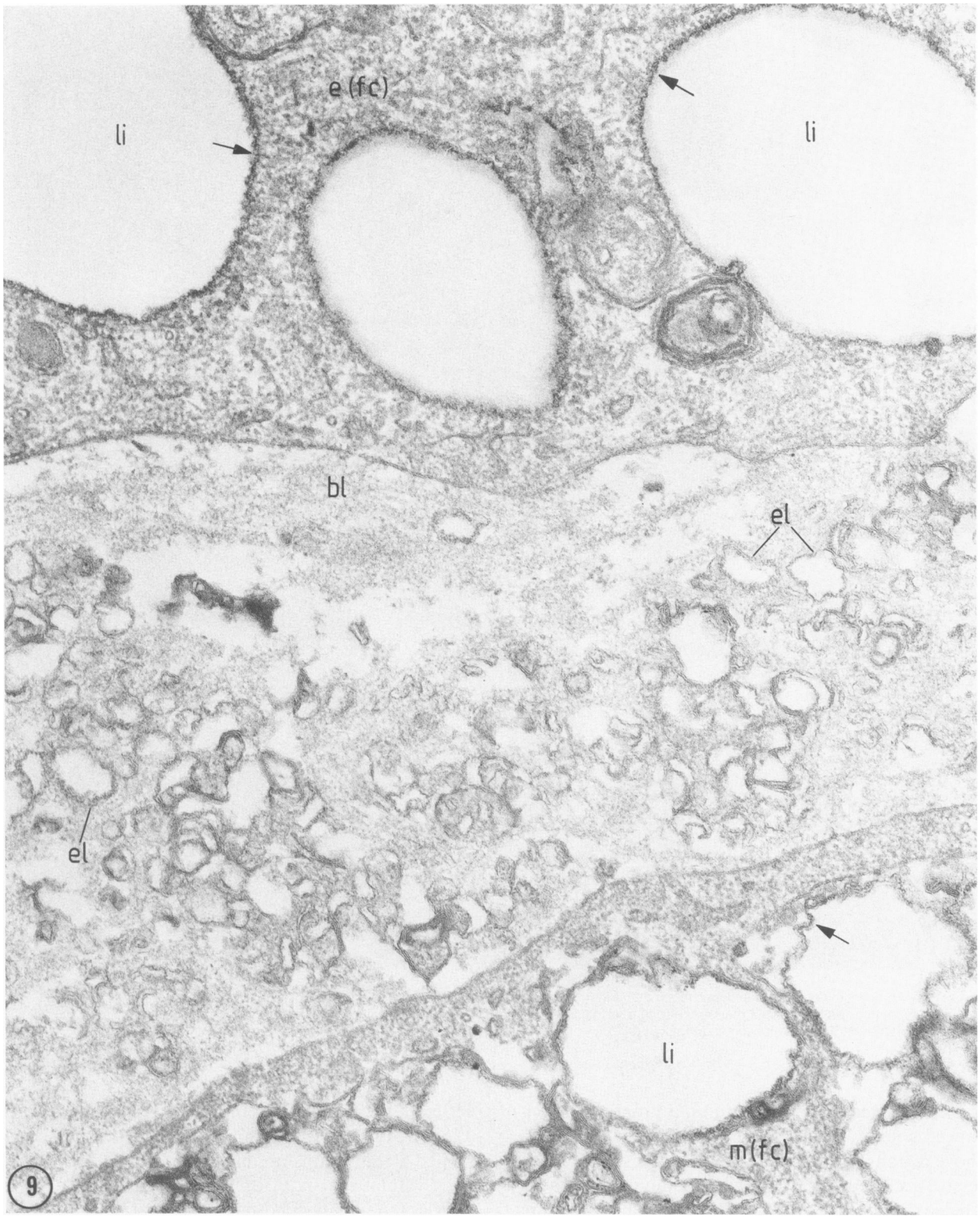

Figure 9—Atrioventricular valve (ventricular aspect) of a hyperlipidemic rabbit at the eighth week of the diet: after incubation with filipin, characteristic deformations (*arrows*) appeared at the periphery of lipid inclusions (*li*) of foam cells (*fc*), as well as in the extracellular liposomes (*el*). Note the difference in the configuration of lipid inclusions in the endothelial cell (*e*) and those in the macrophage-derived foam cell (*m*). *bl*, basal lamina. (×60,000)

Figure 10—Aortic intima of a hyperlipidemic rabbit at the fourth week of the diet; incubation with filipin; freeze-fracture replica. Filipin–sterol complexes (*arrowheads*) appear on the plasma membrane (*pm*) of a foam cell (*fc*) but not on the internal lamellas of their lipid inclusions (*li*). Similar complexes (*arrows*) mark the extracellular liposomes (*el*). (×35,000)

fraction, increases up to 15 times, a progressively enhanced uptake and deposition of lipidic material in the above regions takes place. This is demonstrated by excessive accumulation in the diet-fed animals of radiolabeled dietary cholesterol, radiolabeled β-VLDL, and fluorescent β-VLDL. Though ^{3}H-cholesterol measures both uptake and exchange, the large amounts of cholesterol detected by cytochemistry in the intimal matrix most probably represents accumulation of dietary cholesterol taken up and transcytosed by endothelium. Electron-microscopic examination of the same areas revealed a continuous accumulation within the intimal extracellular matrix of unilamellar and plurilamellar vesicles (presumably phospholipids) containing relatively large amounts of unesterified cholesterol identified by fluorescence microscopy and thin-section and freeze-fracture cytochemistry of specimens incubated with filipin. Because the ELs appear as very smooth surfaces

in freeze-cleaved replicas, they may be very low in or devoid of translamellar proteins (Figure 5). ELs are closely packed, especially in regions rich in proliferated proteoglycans and microfibrils. The number of ELs continues to increase markedly during foam cell formation (Figures 8–10), and they are easily distinguishable in areas free of any visible sign of cytolysis.

The similarity of prelesional changes such as the EL in various locations (eg, aorta, coronary, heart valves) and in different animal species (rabbit and hamster [for the latter, manuscript in preparation]) suggests that a common mechanism is involved. The consistent detection of β-VLDL–gold particles in structures involved in transcytosis, ie, plasmalemmal vesicles[40,41] and to a lesser extent internalized by endocytosis, suggests that transcytosis may be the major process for the transendothelial transport of excess lipoproteins in these animals, but a quantitative estimate remains to be determined. Actually, it has been demonstrated that in hypercholesterolemic animals, accumulation of cholesterol into vessel wall or vascular cells is greater than can be accounted for by endocytosis, because the uptake of cholesterol is higher than that of protein, and cholesterol accumulates even in receptor-deficient cells.[42] Such an uptake is largely mediated by a receptor-independent, nonsaturable pathway.[40,41,43] Some investigators claimed that, at least in capillaries, the endothelial uptake of plasma lipoproteins was governed mostly by the size of permeant molecules,[44] and that internal elastica is a major barrier to the lipoprotein influx through the vessel wall.[45]

Our experiments show that in hypercholesterolemic rabbits, lipid deposition in the vessel intima begins with a formation of an extracellular pool organized primarily in unilamellar or multilamellar vesicles, characteristically rich in unesterified cholesterol. There is biochemical evidence that in the initial atherosclerotic lesions there is an increased accumulation of phospholipids[46–50] considered to take part in the defense mechanism of the arterial wall against the sclerogenic effect of cholesterol.[47,51] After the appearance of monocyte-derived macrophages performing a local cholesterol uptake and esterification, deposits of intracellular esterified cholesterol[52] are added to the forming fatty streak.[6] We do not know at this very early prelesional stage how much of extracellular esterified cholesterol, intact LDL or β-VLDL particles, apoprotein B,[53–55] or apoprotein E[56] exists in regions of EL accumulation. In grossly normal human and animal arteries, as well as in advanced atherosclerotic plaques, modified LDL particles have been convincingly demonstrated.[43–55] The excess free cholesterol may be to a degree incorporated also in the cell membrane of endothelial cells or foam cells[52,57]; these cells did show in our preparations densely packed filipin–sterol complexes (Figure 10), but the sampling did not allow a morphometric analysis comparative to controls. In addition to ELs and cell membrane, a relatively small amount of unesterified cholesterol may be associated with collagens and elastin, as demonstrated in human atheroma.[58] The free cholesterol of the atherosclerotic lesions isolated by Katz[58] in the fraction of nonlipid tissue components may represent ELs unspecifically bound to matrix. Recently it was shown that the intracellular and extracellular lipid accumulation was significantly enhanced by lipoprotein interactions with collagens[59] and proteoglycans.[60,61]

ELs may represent the ultrastructural equivalent of the filipin-positive extracellular particles localized by fluorescent microscopy in the human and animal atherosclerotic aorta by Kruth.[20,62,63]

Extracellular vesiclelike structures or polymorphic membranous material in the atherosclerotic arteries have been previously seen by other investigators,[29,64–68] but they have been commonly ascribed to cell debris or precipitated lipoprotein.

In our experimental model, ELs appear as the earliest ultrastructurally detectable change in an intima devoid of other cells and with no indication of cytolysis. EL accumulation is paralleled by a high level of plasma β-VLDL cholesterol, and this lipidic material proved to be of dietary origin.

The mechanism of formation of ELs is so far unclear. In a previous paper[40] we showed that when LDL is perfused *in situ*, then detected immunocytochemically, the particles which reach the subendothelial space are usually much smaller than those found on plasma membrane or within vesicles. Hypothetically, during transcytosis intact or modified lipoproteins might be partially or completely degraded. In hyperlipidemia, among other impaired endothelial functions, there may be a quantitative and qualitative alteration of transcytosis delivering to the interstitial cells excessive amounts of lipoproteins and lipoprotein constituents, among which are phospholipids, cholesterol esters, and free cholesterol. As a local defense reaction, the sclerogenic cholesterol is rendered inoffensive by reassembly into a phospholipid lamellar liquid-crystalline phase.[50,58] Extracellular cholesterol is not in direct contact with the hydrophilic matrix elements but always incorporated in more complex phases such as phospolipid lamellas,[50,58] which are the ELs. Some cholesterol may reassociate with apoprotein B as with any other proteins present in the matrix. Due to its insolubility in phospholipid bilayers, cholesterol ester should be unlikely to occur in ELs. Whether these ELs may constitute directly or indirectly a chemotactic factor for mono-

cytes, and the possible EL involvement in foam cell formation, remains to be investigated.

References

1. Gerrity RG: The role of the monocyte in atherogenesis: I. Transition of blood-borne monocytes into foam cells in fatty lesions. Am J Pathol 1981, 103:181–190
2. Joris I, Zand T, Nunnari JI, Krolikowski FJ, Majno G: Studies on the pathogenesis of atherosclerosis: I. Adhesion and emigration of mononuclear cells in the aorta of hypercholesterolemic rats. Am J Pathol 1983, 113: 341–358
3. Joris I, Billingham ME, Majno G: Human coronary arteries: An ultrastructural search for the early changes of atherosclerosis (Abstr). Fed Proc 1984, 43:710
4. Mazzone T, Jensen M, Chait A: Human arterial wall cells secrete factors that are chemotactic for monocytes. Proc Natl Acad Sci USA 1983, 80:5094–5097
5. Goldstein JL, Brown MS: The low density lipoprotein pathway and its relation to atherosclerosis. Ann Rev Biochem 1977, 46:897–930
6. Shio H, Haley NJ, Fowler S: Characterization of lipid-laden aortic cells from cholesterol-fed rabbits: III. Intracellular localization of cholesterol and cholesteryl esters. Lab Invest 1979, 41:160–167
7. Mahley RW, Innerarity TL, Brown MS, Ho YK, Goldstein JL: Cholesteryl ester synthesis in macrophages: stimulation by β- very low density lipoproteins from cholesterol-fed animals of several species. J Lipid Res 1980, 21:970–980
8. Clevidence BA, Morton RE, West G, Dusek DM, Hoff HF: Cholesterol esterification in macrophages: Stimulation by lipoproteins containing apo B isolated from human aortas. Arteriosclerosis 1984, 4:196–207
9. Majno G, Joris I, Zand T: Atherosclerosis: New horizons. Human Pathol 1985, 16:3–5
10. Havel RJ, Eder HA, Bragdon IH: The distribution and chemical composition of ultracentrifugally separated lipoproteins in human serum. J Clin Invest 1955, 34:1345–1353
11. Redgrave TG, Roberts DCK, West CE: Separation of plasma lipoproteins by density-gradient ultracentrifugation. Anal Biochem 1975, 65:42–49
12. McFarlane AS: Efficient trace-labeling of proteins with iodine. Nature 1958, 185:53–54
13. Pitas RE, Innerarity I, Weinstein JN, Mahley RW: Acetoacetylated lipoproteins used to distinguish fibroblasts from macrophages in vitro by fluorescence microscopy. Arteriosclerosis 1981, 1:177–185
14. Greenspan P, Mayer EP, Fowler SD: Nile red: a selective fluorescent stain for intracellular lipid droplets. J Cell Biol 1985, 100:965–973
15. Simionescu N, Simionescu M: Galloyl-glucose of low molecular weight as mordants in electron microscopy. J Cell Biol 1976, 70:608–621
16. Simionescu N, Simionescu M, Palade GE: Permeability of intestinal capillaries: Pathways followed by dextrans and glycogens. J Cell Biol 1972, 53:365–392
17. Separd N, Mitchell N: The localization of proteoglycans by light and electron microscopy using safranin O: A study of epiphiseal cartilage. J Ultrastr Res 1976, 54:451–460
18. Adams CWM, Bayliss OB: Lipid histochemistry: Techniques of Biochemical and Biophysical Morphology. Vol. 2. Edited by D Glick, RM Rosenbaum. New York, John Wiley and Sons, 1975, pp 262–267
19. Van Geut CM, Emeis II: Histochemistry of free and esterified cholesterol in human atherosclerotic arteries. Prog Biochem Pharmacol 1977, 14:262–267
20. Kruth HS: Filipin-positive, oil red O-negative particles in atherosclerotic lesions induced by cholesterol feeding. Lab Invest 1983, 50:87–93
21. Bittman R, Fischkoff SA: Fluorescence studies on the binding of the polyene antibiotics filipin III, amphotericin B, nystatin, and lagosin to cholesterol. Proc Natl Acad Sci USA 1972, 69:3795–3799
22. Börnig H, Geyer G: Staining of cholesterol with the fluorescent antibiotic "filipin." Acta Histochem 1974, 50:110–116
23. Friend DS, Bearer EL: β-hydrosysterol distribution as determined by freeze-fracture cytochemistry. Histochem J 1981, 13:535–546
24. McGill HC Jr: Fatty streaks in the coronary arteries and aorta. Lab Invest 1968, 18:560–564
25. Faggiotto A, Ross R, Harker L: Studies of hypercholesterolemia in the nonhuman primate: I. Changes that lead to fatty streak formation. Arteriosclerosis 1984, 4:323–340
26. Insull W, Bartsch GE: Cholesterol, triglyceride and phospholipid content of intima, media and atherosclerotic fatty streak in human thoracic aorta. J Clin Invest 1966, 45:513–523
27. Katz SS, Small DM: Isolation and partial characterization of the lipid phases of human atherosclerotic plaques. J Biol Chem 1980, 255:9753–9759
28. Small DM: Cellular mechanisms for lipid deposition in atherosclerosis. N Engl J Med 1977, 297:873–877
29. Ross R, Harker L: Hyperlipidemia and atherosclerosis: Chronic hyperlipidemia initiates and maintains lesions by endothelial cell deformation and lipid accumulation. Science 1976, 193:1094–1100
30. Ross R: Atherosclerosis: A problem of the biology of arterial wall cells and their interactions with blood components. Arteriosclerosis 1981, 1:293–311
31. Ross R, Bowen-Pope D, Raines EW, Faggiotto A: Endothelial injury: Blood-vessel wall interactions. Ann NY Acad Sci 1982, 401:260–264
32. Florentin RA, Nam SC, Lee KT, Lee KJ, Thomas WA: Increased mitotic activity in aortas of swine, after three days of cholesterol feeding. Arch Pathol 1969, 88:463–469
33. Bell FP, Adamson IL, Schwartz CJ: Aortic endothelial permeability to albumin: Focal and regional patterns of uptake and transmural distribution of ^{131}I-albumin in the young pig. Exp Mol Pathol 1974, 29:57–68
34. Hansson GK, Bondjers G, Bylock A, Hjalmarsson L: Ultrastructural studies on the localization of IgG in the aortic endothelium and subendothelial intima of atherosclerotic and nonatherosclerotic rabbits. Exp Mol Pathol 1980, 33:302–315
35. Weber G, Fabrini P, Resi L: On the presence of a concanavalin A-reactive coat over the endothelial surface and its modifications during early experimental cholesterol atherogenesis in rabbits. Virchows Arch [Pathol Anat] 1973, 359:299–307
36. Gerrity RG, Schwartz CJ: Endothelial cell injury in early mild hypercholesterolemia. Prog Biochem Pharmmacol 1977, 14:213–219
37. Lewis JC, Taylor RG, Jones ND, St. Clair RW, Cornhill JF: Endothelial surface characteristics in pigeon coronary artery atherosclerosis: I. Cellular alterations during the initial stages of dietary cholesterol challenge. Lab Invest 1982, 46:123–138
38. Trillo AA, Prichard RW: Early endothelial changes in experimental primate atherosclerosis. Lab Invest 1979, 41:294–302
39. Ingerman-Wojenski CM, Sedar AW, Nissenbaum M, Silver MJ, Klurfeld DM, Kritchevsky D: Early morphological changes in the endothelium of a peripheral artery of rabbit fed an atherogenic diet. Exp Mol Pathol 1983, 38:48–60
40. Vasile E, Simionescu M, Simionescu N: Visualization of

the binding, endocytosis, and transcytosis of low density lipoprotein in the arterial endothelium in situ. J Cell Biol 1983, 96:1677–1689
41. Vasile E, Simionescu N: Transcytosis of low density lipoprotein through vascular endothelium, Glomerular Disfunction and Biopathology of the Vessel Wall. Edited by A Copley, Y Hamashima, S Seno, M Ventkatachalam. Tokyo, Academic Press (In press)
42. Fielding CJ: The origin and properties of free cholesterol potential gradients in plasma, and their relation to atherogenesis. J Lipid Res 1984, 25:1624–1628
43. Wiklund O, Carew TE, Steinberg D: Role of the low density lipoprotein receptor in penetration of low density lipoprotein into rabbit aortic wall. Arteriosclerosis 1985, 5:135–141
44. Robinson CS, Wagner RC: Differential endocytosis of lipoproteins by capillary endothelial vesicles. Microcirc Endoth Lymph 1985, 2:313–329
45. Smith EB, Staples EM: Distribution of plasma proteins across the human aortic wall: Barrier functions of endothelium and internal elastic lamina. Atherosclerosis 1980, 37:579–590
46. Shore ML, Zilversmit DB, Ackerman RF: Plasma phospholipid deposition and aortic phospholipid synthesis in experimental atherosclerosis. Am J Physiol 1955, 181: 527–531
47. Adams CWM, Bayliss OB, Ibrahim MZM: The distribution of lipids and enzymes in the aortic wall in dietary rabbit atheroma and human atherosclerosis. J Pathol Bacteriol 1963, 86:421–530
48. Zilversmit DB: Mechanisms of cholesterol accumulation in artery wall. Am J Cardiol 1975, 35:559–571
49. Barenholz Y, Gatt S: Sphingomyelin: Metabolism, chemical synthesis, chemical and physical properties, Phospholipids. Edited by JN Hawthorne, GB Ansell. Amsterdam, Elsevier Biomedical Press, 1982, pp 129–177
50. Small DM, Shipley GG: Physical-chemical basis of lipid deposition in atherosclerosis. Science 1974, 185:222–229
51. Adams CWM, Morgan RS: The effect of saturated and polysaturated lecithins on the resorption of 4-^{14}C-cholesterol from subcutaneous implants. J Pathol Bacteriol 1967, 94:73–76
52. Rapp JH, Connor WE, Lin DS, Inahara T, Porter JM: Lipids of human atherosclerotic plaques and xanthomas: Clues to the mechanism of plaque progression. J Lipid Res 1983, 24:1329–1335
53. Hoff HF, Heideman CL, Gotto AM Jr, Gaubatz JW: Apolipoprotein B retention in the grossly normal and atherosclerotic human aorta. Circ Res 1977, 41:684–690
54. Hoff HF, Gaubatz JW: Isolation, purification, and characterization of a lipoprotein containing apo B from the human aorta. Atherosclerosis 1982, 42:273–297
55. Davis HR, Wissler RW: Apoprotein B quantification in rhesus and cynomologous monkey atherosclerotic lesions. Atherosclerosis 1984, 50:241–252
56. Badimon JJ, Mao S: Evidence of large accumulation of apo E but not apo A-1 in the aortic lesions of cholesterol-fed rabbits (Abstr). Arteriosclerosis 1984, 4:523a
57. Jackson RL, Gotto AM Jr: Hypothesis concerning membrane structure, cholesterol, and atherosclerosis. Atheroscl Rev 1976, 1:1–21
58. Katz SS, Small DM, Smith FR, Dell RB, Goodman DWS: Cholesterol turnover in lipid phases of human atherosclerotic plaque. J Lipid Res 1982, 23:733–737
59. Eskenasy M, Mora R, Simionescu N: In vitro study of low density lipoprotein-collagen interaction. Morphol Embryol (Bucur) 1984, 30:147–152
60. Salisbury BG, Falcone DJ, Minick CR: Insoluble low-density lipoprotein–proteoglycan complexes enhance cholesteryl ester accumulation in macrophages. Am J Pathol 1985, 120:6–11
61. Srinivasan SR, Vijayasopal P, Dalferes ER Jr, Abbate B, Radhakrisnamurthy B, Berenson GS: Dynamics of lipoprotein-glycosaminoglycan interactions in the atherosclerotic rabbit aorta in vivo. Biochim Biophys Acta 1984, 793:157–168
62. Kruth HS: Histochemical detection of unesterified cholesterol within human atherosclerotic lesions using the fluorescent probe filipin. Atherosclerosis 1984, 51:281–292
63. Kruth HS, Fry DL: Histochemical detection and differentiation of free and esterified cholesterol in swine atherosclerosis using filipin. Exp Mol Pathol 1984, 40:288–294
64. Ghidoni JJ, O'Neal RM: Recent advances in molecular pathology – a review: Ultrastructure of human atheroma. Exp Mol Pathol 1984, 7:378–400
65. Joris I, Majno G: Cellular breakdown within the arterial wall: An ultrastructural study of the coronary artery in young and aging rats. Virchows Arch [Pathol Anat] 1974, 364:111–127
66. Stebbens WE: Cerebral atherosclerosis: Intimal proliferation and atherosclerosis in the cerebral arteries. Arch Pathol 1975, 99:582–591
67. Stary HC: Coronary artery fine structure in Rhesus monkey: The early atherosclerotic lesion and its progression in primates. Primates Med 1976, 9:359–395
68. Hajjar DP, Wight TN, Smith SC: Lipid accumulation and ultrastructural change within the aortic wall during early spontaneous atherogenesis. Am J Pathol 1980, 100:683–706

Acknowledgments

We are indebted to A. Nistor and A. Hillebrand for monitoring the experimental model. The excellent technical assistance of S. Tancov, E. Florea, F. Georgescu, and M. State (experiments), M. Misici, A. Bitir, M. Mitroaica, and V. Barbulescu (microtomy), E. Stefan and V. Ionescu (photography), M. Schean (graphic work), and M. Mazilu and G. Turcu (editing and typing) is gratefully acknowledged.